

ChemComm

Chemical Communications

www.rsc.org/chemcomm



ISSN 1359-7345



ROYAL SOCIETY
OF CHEMISTRY

COMMUNICATION

Jose Luis Chiara *et al.*

Efficient multi-click approach to well-defined two-faced octasilsesquioxanes: the first perfect Janus nanocube

175
YEARS



Cite this: *Chem. Commun.*, 2016, 52, 5792

Received 28th January 2016,
Accepted 1st March 2016

DOI: 10.1039/c6cc00896h

www.rsc.org/chemcomm

Efficient multi-click approach to well-defined two-faced octasilsesquioxanes: the first perfect Janus nanocube†

Alberto Blázquez-Moraleja,‡^a M. Eugenia Pérez-Ojeda,‡^b José Ramón Suárez,^a M. Luisa Jimeno^c and Jose Luis Chiara*^a

The preparation of the first structurally well-defined Janus nanocube showing two chemically distinct opposed faces is described. The synthetic approach is based on a highly efficient and symmetry-controlled CuAAC functionalization of an octa-azido cubic silsesquioxane with a conformationally constrained tetra-alkyne with an appropriate spatial orientation of the triple bonds.

Named after the two-faced Roman god of beginning and ending, doors and gates, the term Janus particle (“Janus grains”) was coined in 1991 by de Gennes¹ in his Nobel lecture on “*Soft Matter*” to define dissymmetric nano-/micro-objects with two distinct sides. This broken (non-centrosymmetric) symmetry confers directionality on each single particle, which may impart unique physicochemical properties to the particle ensemble that generally do not emerge in the case of symmetric particles, thus foretelling very promising potential applications in electrochemistry, sensing, optical imaging, drug delivery, nanoengines, and catalysis. The past decade has witnessed a great progress in the fabrication and study of (sub)micron-sized inorganic and colloidal Janus particles by direct synthesis, by breaking the symmetry of existing particles or by self-assembling smaller particles into higher Janus-type structures.² However, the synthesis of highly monodispersed and structurally well-defined nanometer-sized Janus particles is still today a very challenging undertaking, the majority of examples described so far being restricted to

heterodimers forming snowman or dumbbell-like nanostructures.³ Molecules with cubic symmetry are ideal candidates for developing routes to well-defined, bifunctional “nano-bricks” endowed with a Janus-type topology and chemical functionality.⁴ Among cubic molecules, octasilsesquioxanes are arguably the most versatile, due to their ready availability and facile functionalization of their pendant organic groups.⁵ Pioneering synthesis of Janus-type silsesquioxanes have been attempted from “half-cage” (cyclic tetrasiloxanetetraol) precursors⁶ and by partial functionalization of homo-octafunctional cages.⁷ However, these routes either suffered from reproducibility problems or tended to afford complex statistical mixtures of multifunctionalized cubes that are difficult to separate.⁸ Other examples have been constructed by covalently connecting two different silsesquioxane cages,^{2c,9} which greatly avoid the purification problems, but yield dumbbell-like nanostructures with higher conformational flexibility and larger (and fluctuating) spatial separation between the two sets of functional groups than in a perfect two-faced Janus cube.

Our group has recently shown that readily available octakis(3-azidopropyl)octasilsesquioxane (**1**)¹⁰ (Fig. 1) can be selectively mono-functionalized in high yield with a variety of terminal alkynes through a stoichiometry-controlled, ligand-accelerated CuAAC reaction to yield structurally well-defined hetero-bifunctional octasilsesquioxane cubes, without formation of polysubstituted products.¹¹ These bifunctional building blocks having orthogonally

^a Instituto de Química Orgánica General, IQOG-CSIC, Juan de la Cierva 3, 28006 Madrid, Spain. E-mail: jl.chiara@csic.es

^b Instituto de Química-Física “Rocasolano”, IQFR-CSIC, Serrano 119, 28006 Madrid, Spain

^c Centro Nacional de Química Orgánica “Manuel Lora Tamayo”, CENQUIOR-CSIC, Juan de la Cierva 3, 28006 Madrid, Spain

† Electronic supplementary information (ESI) available: Synthetic details, full characterization data of the new compounds (multinuclear 1D and 2D NMR spectra and HPLC-MS profiles of the reaction products), and details of the dynamic NMR study and modelling calculations of **5**. See DOI: 10.1039/c6cc00896h

‡ These authors have contributed equally to this work.

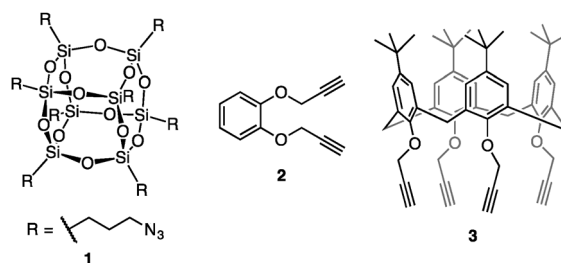
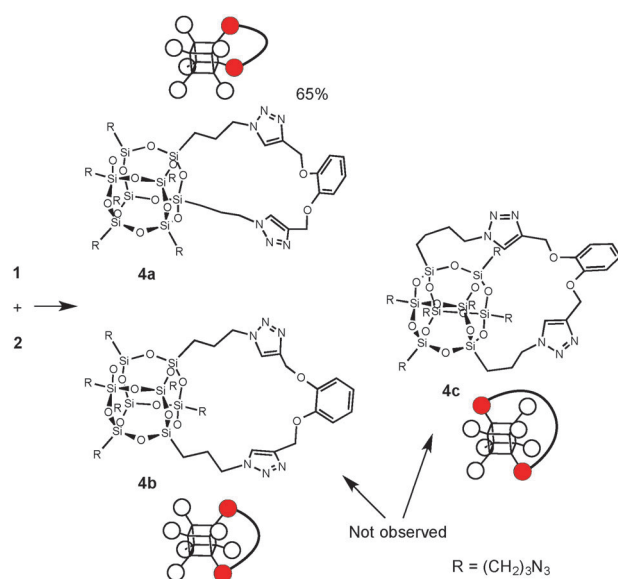


Fig. 1 Structures of the octa-azido silsesquioxane and polyalkynes used in this work.



reactive substituents can be used for the synthesis of symmetric or asymmetric (Janus-type) dumbbell-shaped silsesquioxane dyads and more complex 3D constructs.¹² Based on this previous work, we describe herein an efficient route to heterosubstituted cubic silsesquioxanes, including a Janus-type system, by simultaneous click multifunctionalization with an almost perfect control of regioselectivity. To this end, we have employed tethered polyalkynes **2**¹³ and **3**¹⁴ (Fig. 1), which are conformationally constrained and present an appropriate symmetry and relative spatial distribution of the triple bonds.

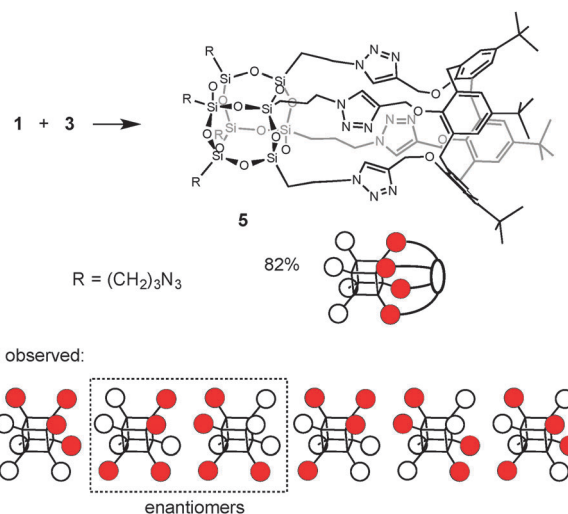
Using our previously optimized “click” conditions,^{10a,11,15} the CuAAC reaction of **2** with a 5-fold molar excess of **1** using [Cu(C₁₈tren)]Br¹⁶ as catalyst in toluene at 50 °C afforded the corresponding “on-edge” bis-triazolyl silsesquioxane **4a** in 65% yield (Scheme 1), accompanied by minor amounts of two dimeric silsesquioxane products (see ESI† for details), as determined by HPLC-ESI analysis of the reaction crude. None of the possible “face-diagonal” nor “cube-diagonal” regioisomers **4b** and **4c**, respectively, could be detected in the reaction crude by HPLC-ESI analysis in spite of the fact that both regioisomers are geometrically and energetically attainable. The observed regioselectivity of this click annulation reaction was much higher than that expected on a purely statistical basis (**4a/4b/4c** = 3 : 3 : 1) for a stepwise click process. This probably reflects the higher kinetic constant of the intramolecular cycloaddition that forms the smallest ring. In addition, the alternative pathways leading to **4b** and **4c** are expected to have lower kinetic constants due to unfavorable interactions with an increased number of neighboring silicon chains interposed between the cyclization termini. The structure of **4a** could be readily assigned by a combination of HRMS spectrometry and multinuclear 1D and 2D NMR spectroscopy (see ESI†). In particular, the 2 : 1 : 1 intensity pattern distribution of the ²⁹Si NMR signals confirmed the regiochemistry of **4a** from molecular symmetry considerations.¹⁷



Scheme 1 Reaction conditions: **2** (0.2 equiv.), [Cu(C₁₈tren)]Br, iPr₂NEt, toluene, 50 °C, 20 h.

After having successfully attained the simultaneous di-functionalization of **1**, we next assayed the corresponding tetra-functionalization with tetraalkyne **3**. As in the previous case, this multi-click transformation is expected to occur through a stepwise process. Considering the symmetry of both reagents, the relative spatial arrangement of the alkyne groups in **3**, and the high on-edge selectivity observed for the di-functionalization of **1** with the parallelly-oriented dialkyne **2**, we anticipated that the tetra-click reaction should proceed with very high “on-face” selectivity. Thus, after the initial intermolecular mono-click attachment of both reagents, the subsequent intramolecular cycloaddition steps are expected to proceed with increasing “on-edge” selectivity for both partners due to the growing conformational restriction of the forming adduct, to finally yield the tetrasubstituted silsesquioxane with very high or complete “on-face” selectivity. In line with these predictions, the reaction of **1** and **3** using the same optimized conditions as above afforded the tetra-triazolyl silsesquioxane **5** in an impressive 82% yield and with complete selectivity, without formation of any of the other six possible regioisomeric tetra-functionalized cubic products (Scheme 2). Again, the structure of **5** could be readily assigned by a combination of HRMS spectrometry and multinuclear 1D and 2D NMR spectroscopy (see ESI†). To our knowledge, compound **5** is the first structurally well-defined and fully characterized nanocube with a perfect two-sided (Janus-type) substitution pattern, *i.e.* with two chemically distinct opposed faces.

Interestingly, the ¹H NMR spectra of **5** in CDCl₃ at different temperatures (Fig. 2) are indicative of a dynamic conformational equilibrium in this molecule. At 25 °C, two separate sets of signals with very different half-widths (Fig. 2b) are observed. The set with sharper signals corresponds to the hydrogens of the four “unreacted” (CH₂)₃N₃ chains of the silsesquioxane moiety (multiplets at 3.28, 1.71 and 0.79 ppm) and the inter-ring bridging methylene groups of the calix[4]arene system (two doublets at 4.30 and 3.25 ppm). The later correlate with a single ¹³C peak at 31.6 ppm in the ¹H/¹³C HSQC spectrum that confirms the



Scheme 2 Reaction conditions: **3** (0.2 equiv.), [Cu(C₁₈tren)]Br, iPr₂NEt, toluene, 50 °C, 20 h.



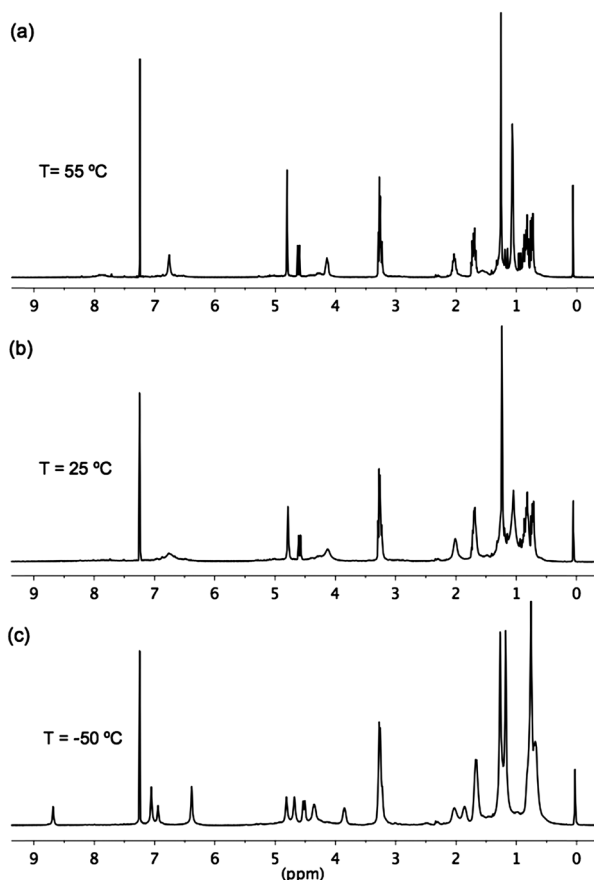


Fig. 2 ^1H NMR spectra (400 MHz) of **5** in CDCl_3 at different temperatures.

expected cone conformation of the calixarene system in **5**.¹⁸ The remaining signals were considerably broadened and included the aromatic and *tert*-butyl protons of the calixarene and the protons of the four linking branches connecting the oxygen atoms of the calixarene to the silicon atoms of the silsesquioxane cube. Increasing the temperature to 55 °C sharpened the spectrum (Fig. 2a), which appeared to be compatible with the expected (time-averaged) C_{4v} molecular symmetry of a perfect Janus cube, although the triazole proton signal still showed a considerable broadening at this temperature. Lowering the temperature to -50 °C led to splitting of all the broadened signals into pairs of equal intensity (Fig. 2c), which were compatible with a C_{2v} molecular symmetry. As previously reported for other tetrasubstituted calix[4]arenes, this coalescence behavior and the observed shielding of half of the aromatic hydrogens (two singlets of equal intensity at 6.40 and 7.07 ppm) at low temperatures provided evidence for the existence of a dynamic equilibrium between two equivalent pinched-cone conformers¹⁹ of the calixarene fragment in this molecule with a C_{2v} symmetry. The conformers interconvert in solution *via* a C_{4v} symmetrical cone transition-state, which corresponds to the time-averaged structure observed in the ^1H NMR spectrum at high temperature. This conformational movement is mechanically transmitted to the linking branches connecting the calixarene to the silsesquioxane cube, which explains the split pattern of signals observed also for the

corresponding protons. The splitting was particularly remarkable for the triazole protons, which appeared as a strongly shielded singlet at 6.95 and a strongly deshielded singlet at 8.69 ppm at -50 °C ($\Delta\delta = 1.74$ ppm).²⁰ In order to obtain the activation barrier for this conformational equilibrium, rate constants were determined from the ^1H NMR spectra over the temperature range 223–323 K (see ESI† for details). The values obtained for $\Delta H^\ddagger = 7.2$ kcal mol⁻¹ and $\Delta S^\ddagger = -19.6$ cal mol⁻¹ K⁻¹ are within the range of those described for the equilibrium between pinched-cone conformers in other calix[4]arenes.¹⁹ The fact that almost identical rate constants were obtained using different proton signals in the lineshape analysis is a clear evidence for the coupled conformational movement of the calixarene and the branches that connect it to the silsesquioxane.

In an attempt to understand the observed conformational equilibrium and the large chemical shift separation between the two types of triazole protons observed in the ^1H NMR spectrum at low temperature, we have carried out a simple molecular modeling study of **5** in vacuum (see ESI† for details). The minimum energy conformer optimized using the semi-empirical PM3 method (Fig. 3) showed the required C_{2v} symmetry observed in the NMR studies at low temperature, with the calixarene in a pinched-cone conformation (see Fig. 3, right view). In this structure, the calixarene is connected to the silsesquioxane core through two alternated pairs of linking chains: one pair with staggered propyl chains bonded to the parallel oriented aryl rings of the pinched cone; the other pair, with propyl chains in a $\text{SiCH}_2\text{-CH}_2\text{C}$ gauche conformation and bonded to the flattened oriented aryl rings. In the latter case, the triazole hydrogen (see the triazole rings that are closer to the C_2 symmetry axis in Fig. 3) is disposed under the center of the triazole ring of the non-equivalent vicinal chain, which will expose it to ring current effects that shield its ^1H NMR signal. In the other pair of linking branches, the triazole hydrogen points to the triazole ring of the non-equivalent chain, which will deshield its proton signal, thus explaining the observed ^1H NMR. Dynamic exchange between the two equivalent pinched-cone conformers of the calixarene system simultaneously interconverts both sets of alternating linking chains.

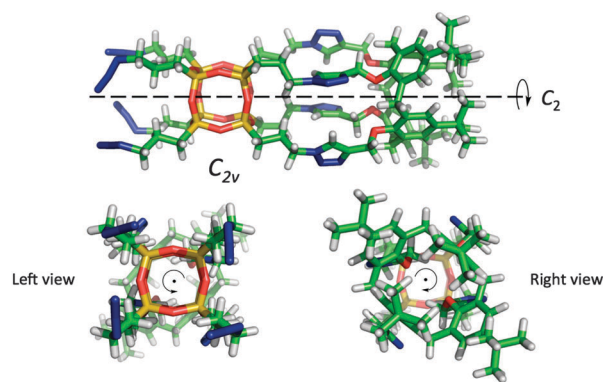


Fig. 3 Minimum energy conformer of **5** optimized using the semiempirical PM3 method, showing the observed C_{2v} symmetry with the calixarene in a pinched-cone conformation.



In conclusion, we have described the synthesis of the first Janus nanocube having two chemically distinct opposed faces. The approach is based on a symmetry-controlled multi-click functionalization of an octa-azido octasilsesquioxane with a tethered tetra-alkyne reagent having an appropriate symmetry and spatial orientation and distribution of the triple bonds. This compound is ready for further functionalization on its tetra-azide face with a diverse array of terminal alkynes to enhance its functional utility, which could be used to modulate its solubility in organic or aqueous solvents and self assembling properties or to prepare it for selective attachment to appropriate surfaces or particles with an expected tight packing thanks to its cuboid-type structure. The presence of the calixarene system and the imposed preorganization of the triazole rings by their covalent attachment to the calixarene and the silsesquioxane cage, together with their known metal and anion complexation properties,²² enables to envisage promising applications for this Janus-type hybrid construct as selective molecular sensor for ion and biomolecular recognition. Work is in progress in our group for the preparation of related systems that could allow the selective detachment of the calixarene to afford a Janus cubic silsesquioxane with two sets of orthogonally reactive functional groups.

We gratefully acknowledge financial support by the Spanish Ministerio de Ciencia e Innovación (project MAT2010-20646-C04-03) and Ministerio de Economía y Competitividad (project MAT2014-51937-C3-1-P). We also acknowledge the Spanish Ministerio de Economía y Competitividad for a FPI contract to A. B., and CSIC for a JAEDOC contract to J. R. S. and a JAEPRE contract to M. E. P.-O., and for support of the publication fee by the CSIC Open Access Publication Support Initiative through its Unit of Information Resources for Research (URICI).

Notes and references

§ The intermolecular functionalization of a cubic octasilsesquioxane using a 4 : 1 stoichiometric mixture of functionalization reagent relative to starting cube will statistically produce the tetra-functionalized product in a maximum yield of 27%, accompanied by smaller amounts of other multisubstituted cubes and a trace amount of unreacted cube (ref. 11b). The tetrasubstituted product is in fact a mixture of seven different cubic regioisomers, including a pair of enantiomers (Scheme 2). Assuming that each of these isomers is formed with equal probability, it follows that the Janus-type one will be produced in <4% yield.

¶ The bis-cycloaddition reaction changes the symmetry of the molecule from O_h in the initial octa-azide **1** to C_{2v} in the final bis-triazolyl product **4a**.

|| The triazolyl hydrogen appears at 7.84 ppm in $CDCl_3$ at room temperature in similar, but conformationally unrestricted, triazolyl derivatives of **3** (ref. 21).

- 1 P. G. De Gennes, *Angew. Chem.*, 1992, **104**, 856–859.
- 2 (a) F. Wurm and A. F. M. Kilbinger, *Angew. Chem., Int. Ed.*, 2009, **48**, 8412–8421; (b) S. Jiang, Q. Chen, M. Tripathy, E. Luijten, K. S. Schweizer and S. Granick, *Adv. Mater.*, 2010, **22**, 1060–1071; (c) Y. Li, W.-B. Zhang, I. F. Hsieh, G. Zhang, Y. Cao, X. Li, C. Wesdemiotis, B. Lotz, H. Xiong and S. Z. D. Cheng, *J. Am. Chem. Soc.*, 2011, **133**, 10712–10715; (d) G. Loget and A. Kuhn, *J. Mater. Chem.*, 2012, **22**, 15457–15474; (e) A. Walther and A. H. E. Mueller, *Chem. Rev.*, 2013, **113**, 5194–5261; (f) X. Pang, C. Wan, M. Wang and Z. Lin, *Angew. Chem., Int. Ed.*, 2014, **53**, 5524–5538; (g) Y. Song and S. Chen, *Chem. – Asian J.*, 2014, **9**, 418–430.
- 3 (a) C. Wang and C. Xu, *Janus particle synthesis, self-assembly and applications*, The Royal Society of Chemistry, 2012, pp. 29–53; (b) H. Liu, C.-H. Hsu, Z. Lin, W. Shan, J. Wang, J. Jiang, M. Huang, B. Lotz, X. Yu, W.-B. Zhang, K. Yue and S. Z. D. Cheng, *J. Am. Chem. Soc.*, 2014, **136**, 10691–10699.
- 4 E. R. Chan, X. Zhang, C.-Y. Lee, M. Neurock and S. C. Glotzer, *Macromolecules*, 2005, **38**, 6168–6180.
- 5 (a) P. D. Lickiss and F. Rataboul, *Adv. Organomet. Chem.*, 2008, **57**, 1–116; (b) D. B. Cordes, P. D. Lickiss and F. Rataboul, *Chem. Rev.*, 2010, **110**, 2081–2173; (c) D. B. Cordes and P. D. Lickiss, *Adv. Silicon Sci.*, 2011, **3**, 47–133; (d) R. M. Laine and M. F. Roll, *Macromolecules*, 2011, **44**, 1073–1109; (e) K. Tanaka and Y. Chujo, *J. Mater. Chem.*, 2012, **22**, 1733–1746.
- 6 (a) K. A. Andrianov, V. S. Tikhonov, G. P. Makhneva and G. S. Chernov, *Bull. Acad. Sci. USSR, Div. Chem. Sci.*, 1973, **22**, 928; (b) M. Z. Asuncion, M. Ronchi, H. Abu-Seir and R. M. Laine, *C. R. Chim.*, 2010, **13**, 270–281; (c) S. Tateyama, Y. Kakihana and Y. Kawakami, *J. Organomet. Chem.*, 2010, **695**, 898–902.
- 7 R. M. Laine, M. Roll, M. Asuncion, S. Sulaiman, V. Popova, D. Bartz, D. J. Krug and P. H. Mutin, *J. Sol-Gel Sci. Technol.*, 2008, **46**, 335–347.
- 8 For selected recent examples on the partial multifunctionalization of octasilsesquioxanes, see: (a) Y. Li, K. Guo, H. Su, X. Li, X. Feng, Z. Wang, W. Zhang, S. Zhu, C. Wesdemiotis, S. Z. D. Cheng and W.-B. Zhang, *Chem. Sci.*, 2014, **5**, 1046–1053; (b) S. Wang, S. Guang, H. Xu and F. Ke, *RSC Adv.*, 2015, **5**, 1070–1078; (c) X.-M. Wang, Q.-Y. Guo, S.-Y. Han, J.-Y. Wang, D. Han, Q. Fu and W.-B. Zhang, *Chem. – Eur. J.*, 2015, **21**, 15246–15255.
- 9 K. Wu, M. Huang, K. Yue, C. Liu, Z. Lin, H. Liu, W. Zhang, C.-H. Hsu, A.-C. Shi, W.-B. Zhang and S. Z. D. Cheng, *Macromolecules*, 2014, **47**, 4622–4633.
- 10 (a) B. Trastoy, M. E. Perez-Ojeda, R. Sastre and J. L. Chiara, *Chem. – Eur. J.*, 2010, **16**, 3833–3841; (b) S. Fabritz, D. Heyl, V. Bagutski, H. Xu and F. Ke, *RSC Adv.*, 2015, **5**, 1070–1078; (c) X.-M. Wang, J. J. Schneider, O. Avrutina and H. Kolmar, *Org. Biomol. Chem.*, 2010, **8**, 2212–2218.
- 11 (a) M. E. Perez-Ojeda, B. Trastoy, I. Lopez-Arbeloa, J. Banuelos, A. Costela, I. Garcia-Moreno and J. L. Chiara, *Chem. – Eur. J.*, 2011, **17**, 13258–13268; (b) M. E. Perez-Ojeda, B. Trastoy, A. Rol, M. D. Chiara, I. Garcia-Moreno and J. L. Chiara, *Chem. – Eur. J.*, 2013, **19**, 6630–6640.
- 12 X. Wang, Y. Yang, P. Gao, D. Li, F. Yang, H. Shen, H. Guo, F. Xu and D. Wu, *Chem. Commun.*, 2014, **50**, 6126–6129.
- 13 B. Venugopalan and K. K. Balasubramanian, *Heterocycles*, 1985, **23**, 81–92.
- 14 E.-H. Ryu and Y. Zhao, *Org. Lett.*, 2005, **7**, 1035–1037.
- 15 B. Trastoy, D. A. Bonsor, M. E. Perez-Ojeda, M. L. Jimeno, A. Mendez-Ardoy, J. M. Garcia-Fernandez, E. J. Sundberg and J. L. Chiara, *Adv. Funct. Mater.*, 2012, **22**, 3191–3201.
- 16 (a) G. Barre, D. Taton, D. Lastecoueres and J.-M. Vincent, *J. Am. Chem. Soc.*, 2004, **126**, 7764–7765; (b) N. Candelon, D. Lastecoueres, A. K. Diallo, J. Ruiz Aranzaes, D. Astruc and J.-M. Vincent, *Chem. Commun.*, 2008, 741–743.
- 17 B. J. Hendan and H. C. Marsmann, *J. Organomet. Chem.*, 1994, **483**, 33–38.
- 18 C. Jaime, J. De Mendoza, P. Prados, P. M. Nieto and C. Sanchez, *J. Org. Chem.*, 1991, **56**, 3372–3376.
- 19 M. Conner, V. Janout and S. L. Regen, *J. Am. Chem. Soc.*, 1991, **113**, 9670–9671.
- 20 S. Cecioni, S. E. Matthews, H. Blanchard, J.-P. Praly, A. Imberty and S. Vidal, *Carbohydr. Res.*, 2012, **356**, 132–141.
- 21 S. Cecioni, S. E. Matthews, H. Blanchard, J.-P. Praly, A. Imberty and S. Vidal, *Carbohydr. Res.*, 2012, **356**, 132–141.
- 22 (a) V. Haridas, S. Sahu, P. P. Praveen Kumar and A. R. Sapala, *RSC Adv.*, 2012, **2**, 12594–12605; (b) B. Schulze and U. S. Schubert, *Chem. Soc. Rev.*, 2014, **43**, 2522–2571.

